

# Automatic Articular Cartilage Segmentation Based on Pattern Recognition from Knee MRI Images

Jianfei Pang · PengYue Li · Mingguo Qiu · Wei Chen ·  
Liang Qiao

Published online: 21 February 2015  
© Society for Imaging Informatics in Medicine 2015

**Abstract** An automatic method for cartilage segmentation using knee MRI images is described. Three binary classifiers with integral and partial pixel features are built using the Bayesian theorem to segment the femoral cartilage, tibial cartilage and patellar cartilage separately. First, an iterative procedure based on the feedback of the number of strong edges is designed to obtain an appropriate threshold for the Canny operator and to extract the bone-cartilage interface from MRI images. Second, the different edges are identified based on certain features, which allow for different cartilage to be distinguished synchronously. The cartilage is segmented preliminarily with minimum error Bayesian classifiers that have been previously trained. According to the cartilage edge and its anatomic location, the speed of segmentation is improved. Finally, morphological operations are used to improve the primary segmentation results. The cartilage edge is smooth in the automatic segmentation results and shows good consistency with manual segmentation results. The mean Dice similarity coefficient is 0.761.

**Keywords** Knee · Articular cartilage · Segmentation · MRI · Pattern recognition

---

Jianfei Pang and PengYue Li contributed equally to this work.

J. Pang · P. Li · M. Qiu (✉)  
Department of Medical Image, College of Biomedical Engineering,  
Third Military Medical University, Chongqing, China  
e-mail: qiumingguo@yahoo.com

W. Chen  
Department of Radiology, Southwest Hospital, Third Military  
Medical University, Chongqing, China

L. Qiao  
Department of Computer Science, College of Biomedical  
Engineering, Third Military Medical University, Chongqing, China

## Introduction

The knee, the most complex and easily damaged joint in the human body, is composed of the femur, tibia, patella, ligaments, cartilage, and other tissues. Cartilage, a special connective tissue covering the loading surface of the knee, is pressure-resistant, absorbs vibration, diffuses stress, and possesses other favorable mechanical properties. Damage or pathological changes to articular cartilage, such as those caused by osteoarthritis (OA), would restrict movement. Magnetic resonance imaging (MRI) is one of the most important methods for non-invasively evaluating the morphology and function of cartilage in the clinic. The method is helpful in describing and evaluating cartilage quantitatively by calculating morphological parameters (thickness, surface area, volume, etc.) based on accurate cartilage segmentation. Currently, cartilage segmentation is mainly completed manually or semi-automatically by radiologists with image processing software. An experienced radiologist needs at least 30 min to complete segmentation work for one patient. Kapur built a geometry-based model using parameters such as distance and normal vectors to segment the knee cartilage [1]. Ghosh et al. segmented cartilage automatically with a watershed algorithm that could identify normal and pathological cartilage structures [2]. With the development of computer technology and artificial intelligence, pixel-based methods have been combined with pattern recognition, and many algorithms that result in good cartilage segmentation have been developed. Folkesson et al. designed a cartilage pixel classifier based on the k-nearest neighbor method using pixel features for low-field MRI images. In her study, 139 knee joints were examined with T1 sequences, and the mean Dice similarity coefficient (DSC) was determined to be 0.80 [3]. Zhang designed a support vector machine (SVM) model using the gray value of pixels, cartilage thickness, the mean curvature of the boundary, and spatial features for cartilage segmentation, and the

model was validated based on a dataset of multiple MR sequences, including FS SPGR, FIESTA, and IDEAL GRE, whose mean DSC was determined to be 0.913 [4]. Bone is easier to segment than cartilage in knee MRI images, and the cartilage covers the articular surface. Therefore, many researchers employ a stepwise strategy when segmenting cartilage, that is, the bone is segmented first and the cartilage next. For example, Fripp et al. segmented the three main bones (femur, tibia, and patella) first and then extracted the bone-cartilage interface (BCI) that could be used for initialization and constraint of cartilage segmentation using an active shape model. Their framework was validated on data acquired for 20 healthy knees using a FS SPGR MR sequence, and average DSC of 0.83, 0.83, and 0.85 for the patellar, tibial, and femoral cartilage were obtained [5]; other deformable models and improvements thereof have also been used in studies on cartilage segmentation [6, 7].

Geometry-based methods only produce good results for normal cartilage, but these methods are not suited for pathological cartilage or are difficult to use to distinguish the overlapping cartilage that is ever-present in cartilage images. The cartilage edge is not smooth enough in the results segmented by pixel-based methods, and there are often holes or disconnected areas. Thus, herein, a new method based on edge detection and pattern recognition is designed for cartilage segmentation to retain the advantages of both geometry and pixel-based methods and overcome their shortcomings. In this paper, we mainly focus on healthy cartilage segmentation, but this method still has the potential to segment pathological cartilage.

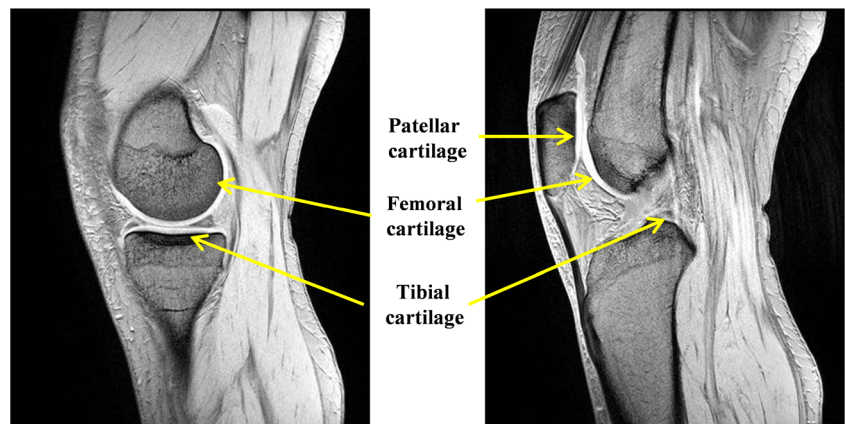
### Image Acquisition and Preprocessing

MRI data were provided by the Department of Radiology, Southwest Hospital, Third Military Medical University. The

data comprised sagittal MRI images of the right knee joints of six healthy volunteers (mean age, 23.3 years; range, 20–25 years). Written consent was obtained from each participant, and the Ethics Committee of the Third Military Medical University approved the protocol. The data were acquired by a 1.5 T SIEMENS scanner with T2-weighted and fat suppression sequences (sagittal slice thickness of 2.5 mm, FOV of  $160 \times 160$  mm,  $384 \times 384$  matrix, TR of 1363 ms, TE of 4.42 ms, flip angle of  $60^\circ$ ). The pixel depth of a DICOM image is 16 bits, which was too large to process in this study; therefore, the images were converted to 8-bit grayscale images using MRIcro software (<http://www.mccauslandcenter.sc.edu/mricro/mricro/>). MRIcro allows for efficient viewing and exporting of MRI images. The window center was set to 731, and the window width was set to 1442 to convert the image to 8 bit with window-leveling algorithm. (The window center refers to the image intensity that will be displayed as a medium gray, and the window width describes the range between bright white and full black). Experienced radiologists manually segmented approximately 100 slices from images obtained from six healthy volunteers. The volunteers were divided into two groups randomly, with each group featuring three cases: one group for training, to estimate the classifier parameter, and the other group for testing, to verify the feasibility and accuracy of our method.

As shown in Fig. 1, there was some noise in the MRI images, especially in the bone tissue, which would greatly affect edge detection; thus, denoising was necessary. A Gaussian low-pass filter (hsize, vsize 5, and standard deviation 2) was used to denoise the converted images. Figure 1 shows two sagittal MRI images of a healthy knee. Femoral cartilage, tibial cartilage, and patellar cartilage are marked by yellow arrows. The gray part is bone tissue and cartilage, and the white narrow part covers the patella, tibia, and femur on the surfaces where the bones contact each other. The knee also contains muscle tissue, connectivum, blood vessels, and other components. Cartilage exhibits a stronger signal than bone

**Fig. 1** MRI images of the knee joint



and exhibits a clear boundary with respect to the surrounding tissue, but it is similar to muscle, which makes it difficult to distinguish.

## Segmentation Method

The BCI (including the bone edge) is easy to identify, and it is helpful to determine the position of cartilage. Therefore, a stepwise strategy was adopted to segment cartilage: The BCI was obtained first, and then, cartilage was segmented. Our cartilage segmentation framework is shown in Fig. 2. First, the strong edges were detected with the Canny operator, and the BCI was obtained. Second, the pixel features (distance from BCI, intensity) were calculated, and the intensity variance of eight neighboring pixels was calculated in the pre-processing images. Third, a Bayesian classifier was used to classify the pixels using distance from the BCI, intensity, position, and variance as features. Finally, the cartilage segmentation results were obtained after post-processing.

### BCI Detection and Recognition

#### Edge Detection Based on Iterative Threshold

The Canny edge detector [8] is an ideal detection operator because of its sensitivity and high signal-to-noise ratio (SNR). An improved self-adaptive threshold Canny detector was used to set the initial gradient threshold ( $T_l, T_h; T_l < T_h$ ) introduced by Huo [9], which combines the advantages of the Otsu method and probability model method to obtain the low threshold  $T_l$  and high threshold  $T_h$  adaptively.  $T_l$  and  $T_h$  are the key parameters for detecting and connecting edges using the Canny detector. The quality of the results obtained using the Canny detector is closely related to the threshold value; a low threshold will generate many weak edges, and a high threshold may not be able to detect the BCI. Thus, the threshold value must be set adaptively based on the premise that BCI can be detected completely, and it is important to set a suitable gradient threshold adaptively, which can greatly

reduce the number of iterations required. The edges of skin, bone, and cartilage were strong in the MRI images; therefore, other weak edges could be removed by setting a higher threshold. The Canny detector was used to extract the edges of the two MRI images, as shown in Fig. 1, and the results are shown in Fig. 3.

The main edges in Fig. 3 are the skin, femur, tibia, patella, and muscle tissue, which have a high gradient. The BCI was detected completely, which contained many pixels and was larger than the majority of other edges. However, the BCI was not always detected completely in all slices. In this case, the cartilage could not be segmented successfully when the edge detection was poor. Thus, further improvement of the threshold setting was required. The BCI was identified as a “strong edge” (many pixels, large area, and high gradient) by edge detection compared to other edges, which could be determined by further detection experiments. Therefore, the threshold could be corrected with the feedback obtained from calculating the number of “strong edges”. This process is illustrated in Fig. 4. With the initial threshold, the number of strong edges was calculated first. When the number was excessively high (e.g., more than 10), the threshold had to be increased and lowered in small increments so that a better edge detection result could be obtained using this adaptive threshold setting. The number of iterations was typically less than 50.

#### Edge Optimization

Other edges were also detected using the adaptive threshold (Fig. 3), e.g., example, muscle tissue, compact bone, and cancellous bone, which resulted in some edges that are broken and coarse, with many “glitches” and short branches. Therefore, we used morphological processing (connected component labels, spur removal, edge connection, and thinning) to improve the results. After the morphological processing of the results shown on the right side of Fig. 3, the optimized results shown in Fig. 5 were obtained.

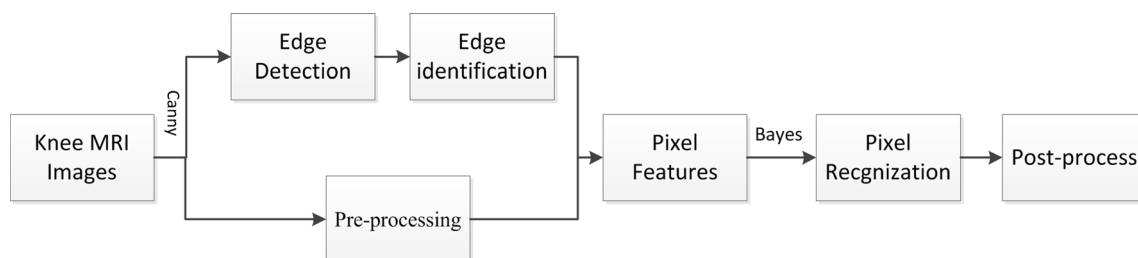
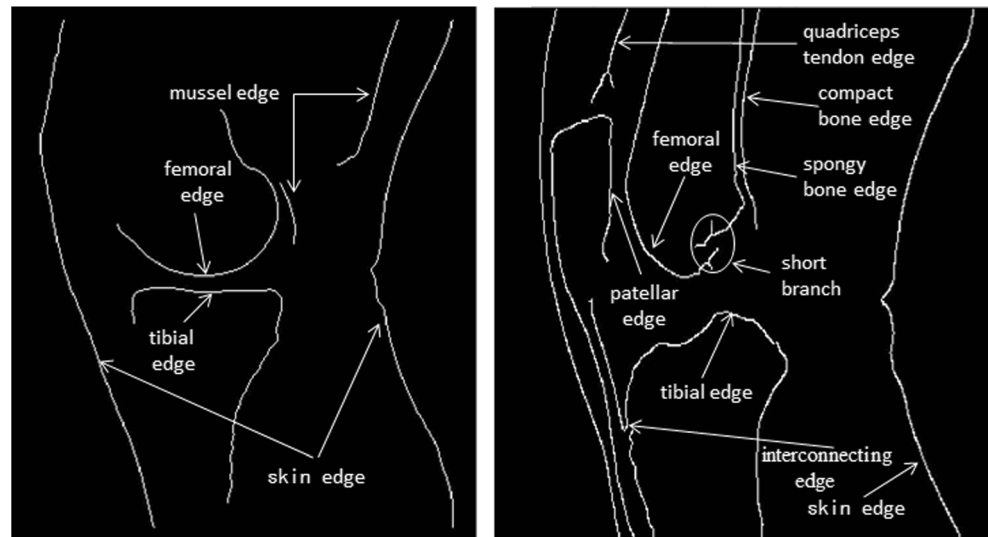


**Fig. 2** The block diagram of the presented segmentation framework

**Fig. 3** Edge detection using Canny detector



Cartilage covers the bearing surface of the knee, and the curvature changes slowly; however, a large part of the BCI extracted by edge detection is not covered by cartilage shown in Fig. 5. Thus, corner detection was used to break the edges [10], which allowed for more accurate BCI detection. The corner detection results are shown in Fig. 6, except for the edge endpoints. There still are two corners that divide the patella edge into three parts. The cartilage only covers the right one, and a similar configuration can be gathered from the edges of the femur and patella. Corners are always detected in areas where the curvature changes fast, where there is no cartilage

coverage; thus, the search space of cartilage is narrowed, and the identification error caused by unrepresentative interconnecting edges is reduced (shown in Fig. 6).

#### *SVM-Based Edge Identification*

The optimized edges include skin, BCI, and other strong edges, and the BCI must be identified first before calculating the distance from the BCI, which separates different cartilage from other edges. If optimized edges are not identified accurately, the cartilage would not be segmented.

**Fig. 4** Flowchart for edge detection based on iterative threshold

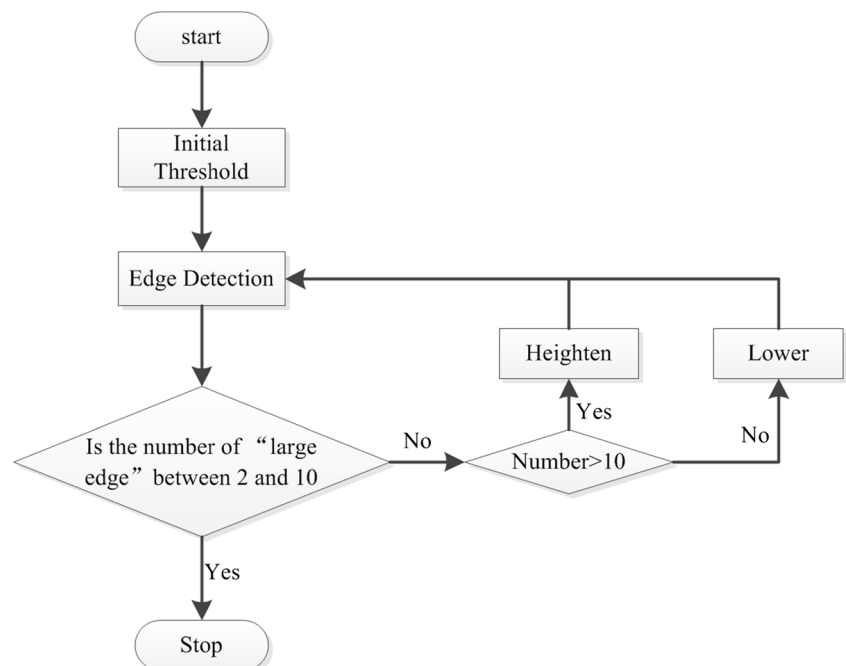




**Fig. 5** Optimized results of edge detection

The edges are classified into six classes (left and right skin, tibial edge, femoral edge, patella edge cartilage, and the other edges). The skin edge has many pixels and a high length-to-width ratio, and each of its sides (left or right) does not have foreground pixels. Similarly, five main features (shown in Table 1) are used to classify the BCI and other edges.

As shown in Table 1, the BCI can be distinguished from other edges by certain features (opening direction, location, number of pixels in the horizontal direction, etc.), which are discussed in detail in a later section. Although some of the short branches are removed by morphological processing, there are still few edges with more than two endpoints; therefore, a contour tracing method involving the eight neighboring pixels is used to obtain the edge sequence and break the multiple-branched edge into a single sequence based on which all features are calculated.

As shown in Fig. 7, the opening direction of an edge sequence is calculated by determining where the intermediate points are located along the line connecting endpoints, which determines whether the opening direction is downward,

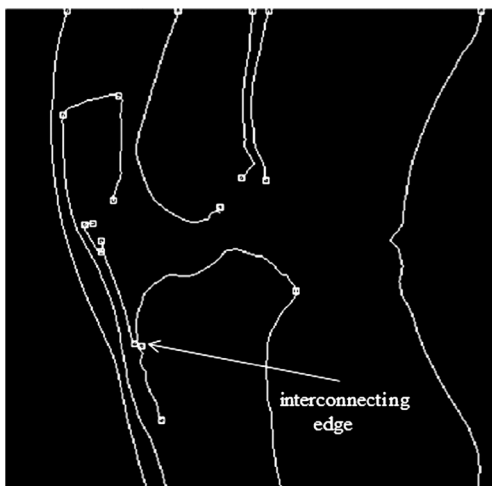


**Fig. 6** Results of corner detection

upward, or straight, and three values are sufficient to recognize the BCI. When the intermediate points are located at a short distance (e.g., 10) from the connecting line of the endpoints, the edge is determined to be straight. The intermediate points are equally selected along the edge. The final value of the opening direction is the ratio of the number of upward, downward, and straight points to the total number of points (20, representing a balance between accuracy and computational efficiency). The location of an edge is the centroid coordinate of a finite set of points in the vertical and horizontal directions [11].

The eight-direction Freeman chain code is calculated first when the number of pixels in the horizontal direction and along a clockwise rotation angle are calculated, as shown in Fig. 8. The horizontal direction is 0 or 4 for the chain code. Thus, the number of pixels in the horizontal direction is the ratio of the chain code number, 0 or 4, to the total number of pixels in a sequence. The clockwise rotation angle is calculated as follows: In the first code direction, calculate the clockwise rotation angle of the chain code, then determine and compare the rotation angle value with that of the next chain code, which is calculated individually. When the angle is greater than  $180^\circ$ , it is considered negative, and the cumulative value of the angle is determined to be the final clockwise rotation angle.

The edges can then be classified via the SVM using the feature vector of each edge. However, the degree of difficulty with which different edges are recognized varies, and the order from high to low degree of difficulty is skin edge, femoral edge, tibial edge, and patella edge. According to this order, the one-versus-one SVM method [12] is used to identify edges. This method trains a classifier after every two classes. Thus, for six classes, the method will train  $6 \times 5 / 2 = 15$  classifiers.

The kernel of the SVM model is a linear function. The edge features previously introduced for classification are determined first. Approximately, 1000 edges obtained from the training set (details in section [Classifier Design](#)) are marked manually as training data, and features that do not range from 0 to 1 are normalized first using a min-max normalization method. The classifiers are trained with the training data. The recognition accuracy is greater than 95 % when the SVM model is used to recognize unknown edges. Most of the recognized incorrectly edges are not the BCI or do not have cartilage coverage, which does not affect the cartilage segmentation procedure.

## Cartilage Segmentation

### Feature Extraction

Based on the experiments and the literature [1, 3], the following features were finally determined for use in pixel classification: the intensity  $f(x,y)$ ; the distance from the BCI  $d(x,y)$



**Table 1** Features' comparison of different edges

Edges	Opening direction	Location	Number of pixel in the horizontal direction	Clockwise rotation angle (°)	Number of pixels
Femoral edge	Up	Upward	Numerous	More than 180	Numerous
Tibial edge	Down	Below	Numerous	More than 180	Numerous
Patella edge	Down	Left-center	Few	More than 90	Few
Left skin edge	straight	Left	Few	Less than 45	Numerous
Right skin edge	straight	Right	Few	Less than 45	Numerous

[1]; the gradient norm determined by the Prewitt operator  $|\nabla f(x,y)|$  and position  $o(x,y)$  [3]; and the intensity variance of the eight neighboring pixels  $\sigma_8(x,y)$ . All features were calculated after denoising by a Gaussian low-pass filter in the section of image preprocessing. The distance from the BCI was the Euclidean distance between each pixel and the corresponding nearest point on the BCI. When a pixel was located inside the bone tissue, the distance was considered to be negative; otherwise, it was considered to be positive. The sign (positive or negative) was calculated by determining whether the point was in the polygonal region of bone formed by the BCI. When a pixel was located near the edge of the patella cartilage, the position was determined to be the horizontal distance between the pixel and the left-most point of the femoral cartilage edge. When a pixel was located near the edge of the femoral cartilage or tibial cartilage, the position was determined to be the vertical distance between the pixel and the lowest end of the femur. The position reflected the relationship between the different types of cartilage in the knee. The distance from the BCI and position could limit the range of pixel classification and was also useful in distinguishing the

contacted cartilage from the muscle tissue close to the cartilage.

### Classifier Design

Pixels were classified into two classes: cartilage and non-cartilage. Femoral cartilage, tibial cartilage, and patellar cartilage classifiers were built separately using the minimum error probability classifier of Bayesian decision theory. The Bayesian classifier only requires a small amount of training data to estimate the parameters necessary for classification and is faster speed and more effective and accurate compared to the SVM. More importantly, the accuracy of the classifier in segmenting our MRI images is higher than that of the SVM, which has been previously tested. Let  $\mathbf{x}=(x_1, x_2, \dots, x_n)$  be the feature vector described in section [Feature Extraction](#), and  $\omega_i$  is a class. If the probability of class membership in  $\omega_1$  is higher than the probability of class membership in  $\omega_2$ , then  $\mathbf{x}$  belongs to  $\omega_1$ ; otherwise,  $\mathbf{x}$  belongs to  $\omega_2$  (see [13] for details).

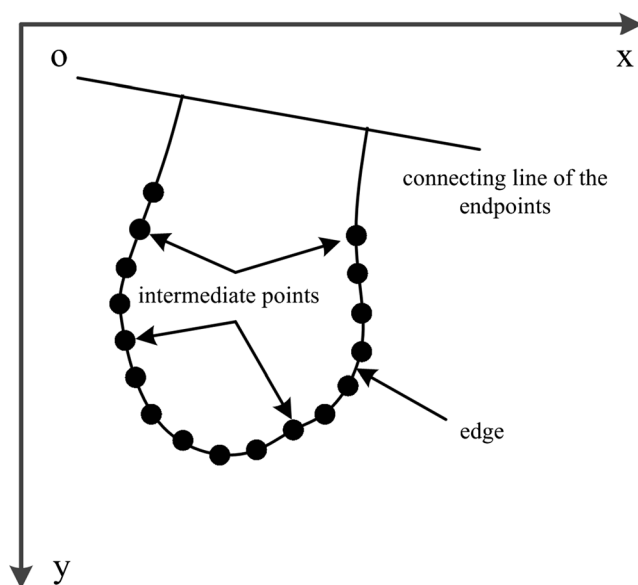
Described mathematically,

$$\text{if } \frac{P(x_1, x_2, \dots, x_n | \omega_i) P(\omega_i)}{P(x_1, x_2, \dots, x_n)} > \frac{P(x_1, x_2, \dots, x_n | \omega_j) P(\omega_j)}{P(x_1, x_2, \dots, x_n)}, i \neq j, \text{ then, } \mathbf{x} \in \omega_i \quad (1)$$

where  $P(x_1, x_2, \dots, x_n | \omega_i)$  is called the class-conditional probability distribution and  $P(\omega_i)$  is the prior probabilities. In practice,  $P(x_1, x_2, \dots, x_n)$  is identical to all classes and therefore can be ignored. In this case, the formula (1) can be rewritten as follows:

$$\text{if } P(x_1, x_2, \dots, x_n | \omega_i) P(\omega_i) > P(x_1, x_2, \dots, x_n | \omega_j) P(\omega_j), i \neq j, \text{ then, } \mathbf{x} \in \omega_i \quad (2)$$

The features are considered to contribute independently to the probability, and a typical assumption is that the features

**Fig. 7** The opening direction of an edge

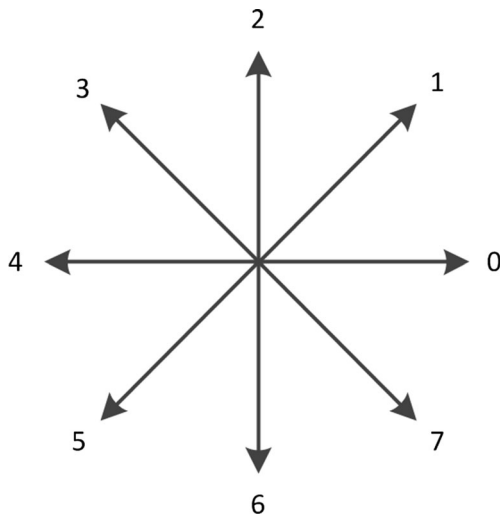


**Fig. 8** The eight-direction Freeman chain code

associated with each class are continuous and distributed according to a Gaussian distribution. Therefore, only the feature parameters (mean and variance in each class) and the prior probabilities  $P(\omega_i)$  need to be obtained to design a classifier. The feature vector is calculated first, but it is time-consuming to calculate all pixels. For example, there are more than 400,000 pixels in one case, which requires approximately 1 h to calculate the feature vector for each pixel. Thus, according to the anatomical features of cartilage, two strategies are used to reduce the number of training pixels, which reduces the computational efficiency by approximately 80 %:

- (1) Whether cartilage is included  
When an image does not have a BCI, there is no need to classify the corresponding cartilage.
- (2) Narrow the search space

Cartilage lies on the surface of bone and has a width of 1–6 mm. Only pixels less than 8 mm from the BCI (includes some non-cartilage pixels) need to be classified.

#### *Pixel Classification and Post-processing*

The same training strategies are used to reduce the number of pixels for classification when the cartilage is segmented with the three Bayesian classifiers. After pixel classification, the segmentation results still contain holes, repeated classifications, non-smooth areas, isolated points, and more than one connected regions, which does not match the anatomical features cartilage. Thus, post-processing is required.

Repeated classification occurs due to contact between some slices of patellar cartilage and femoral cartilage or between femoral cartilage and tibial cartilage. Pixels in these areas would be classified by two classifiers, and the pixels may be classified as two types of cartilage. In this situation,

the pixels are classified into the class with the higher probability. Regarding the holes, non-smooth areas, and isolated points, a morphological operator (when a background pixel has at least five foreground pixels, then the pixel is the foreground pixel) is used. When a segmentation result has many connected regions, the small regions (30 pixels) are removed.

#### **Results**

Approximately 10 min was required to complete the automatic segmentation (30–42 slices) for one case on a standard desktop (Intel(R) Core(TM)2 Duo CPU T6600 @2.2 GHz and 2GB RAM) PC. The automatic segmentation results of three test images are shown in Fig. 9. The edge of the segmented cartilage is smooth, and the contact cartilage was segmented successfully, based on a qualitative analysis.

To make a quantitative comparison between manual segmentation and automatic segmentation, the DSC was calculated, which is the gold standard for evaluating segmentation results, the details of which are discussed in [14].

$$DSC = \frac{2|X \cap Y|}{|X| + |Y|} \quad (3)$$

where  $X$  is the manual segmentation set and  $Y$  is the automatic segmentation set. The numerator is two times the number of pixels at the intersection of  $X$  and  $Y$ , and the denominator represents the number of pixels in  $X$  and  $Y$ . The closer to 1 the value of DSC is, the better the agreement between the two segmentation sets. The DSC values of femoral cartilage (0.84), tibial cartilage (0.78), and patellar cartilage (0.73) are shown in Fig. 10.

The DSC values of these three types of cartilage were all greater than 0.7 (mean, 0.761), which indicates that there was good agreement between the results obtained by our method and those obtained by manual segmentation.

#### **Discussion**

This article described research on a method for automatically segmenting knee articular cartilage in MRI images. The automatic segmentation method is based on pattern recognition and uses a stepwise strategy. First, strong edges in images were detected, and an iterative threshold for a Canny detector and an edge-optimized method were developed. Subsequently, SVM was used to identify edges such that different types of cartilage could be differentiated and the range of cartilage could be defined simultaneously. The initial segmentation was completed by Bayesian minimum error classification. The final segmentation results were obtained by

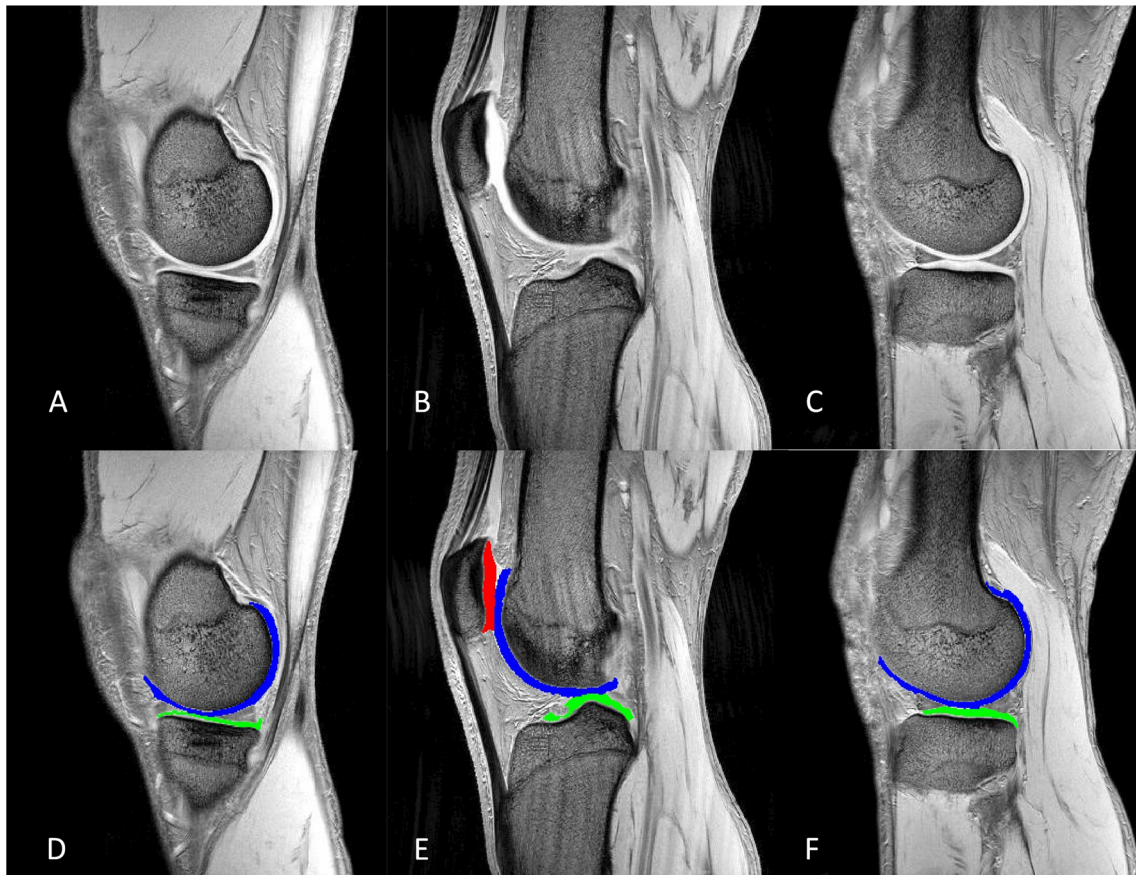


**Fig. 9** Comparison of segmentation results. **a, b, c** original images; **d, e, f** automatic segmentation results

morphological processing of the initial segmentation results. The results obtained by automatic segmentation and those obtained by manual segmentation showed good agreement, as indicated by the mean DSC value of 0.761. Compared with the results of similar cartilage segmentation studies reported in [3–5], the DSC value of patellar cartilage is competitive, whereas the values obtained for tibial and femoral cartilage are not. However, only five features and one MRI sequence were used in this study, which reduced the computational efficiency.

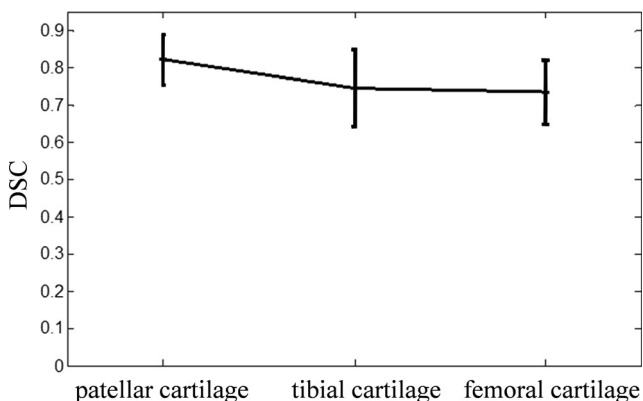


**Fig. 10** DSC values of different types of cartilage

The method proposed by Kapur [1] requires the manual segmentation of bone, which is time-consuming. Using our edge detection and identification method not only reduces the workload but also benefits pixel classification and allows for the differentiation between the three types of cartilage. Compared with the pixel classifier models presented by Jenny and others [3, 4], which suffer from limitations due to the positions of pixels, the detection features used in the proposed method are calculated after the BCI is recognized, which provides more steady performance. Pathological cartilage usually undergoes some morphological changes (thinning, even breaking), which represents a great challenge to the use of deformable models or improvements thereof. The algorithm presented in this article is based on pixel classification and also incorporates anatomical information, and the aforementioned morphological changes do not affect the pathological cartilage segmentation results.

## Conclusion

In summary, this paper described an automatic method for cartilage segmentation using MRI images of the knee. The cartilage edge is smooth in the automatic segmentation results



and shows good consistency with the results of manual segmentation. The main advantages of the proposed method are as follows: (1) The BCI is extracted based on edge detection and recognition rather than bone segmentation; (2) the anatomical information of cartilage has been transformed to pixel features, and all pixel features can be used for pathological cartilage segmentation. The primary limitation of this method is that it has only been validated on a small healthy knee dataset; thus, it is important to analyze data pertaining to pathological cartilage in the future, which can provide quantitative information for the clinical diagnosis of early cartilage lesions and allow for the evaluation of the therapeutic effects of drugs.

**Acknowledgments** This study was sponsored by the National Natural Science Foundation of China (61190122/F0205) and the Natural Science Foundation Project of CQ CSTC (cstc2011jjA10032).

## References

1. Kapur T: Model Based Three Dimensional Medical Image Segmentation. Massachusetts Institute of Technology, Cambridge, 1999, pp 54–70
2. Ghosh S, Beuf O, Ries M, Lane NE, Steinbach LS, Link TM, Majumdar S: Watershed Segmentation of High Resolution Magnetic Resonance Images of Articular Cartilage of the Knee. Proceedings of the 22nd Annual International Conference of the IEEE 4, 2000, pp 3174–3176
3. Folkesson J: Segmenting Articular Cartilage Automatically Using a Voxel Classification Approach. IEEE Trans Med Imaging 26:106–115, 2007
4. Zhang K: Segmenting Human Knee Cartilage Automatically From Multi-contrast MRI Images Using Support Vector Machines and Discriminative Random Fields. IEEE International Conference on Image Processing, 2011, pp 721–724
5. Fripp J: Automatic Segmentation and Quantitative Analysis of the Articular Cartilages From Magnetic Resonance Images of the Knee. IEEE Trans Med Imaging 29:56–65, 2010
6. Tejos C, Hall L D, Cardenas-Blanco A: Segmentation of Articular Cartilage Using Active Contours and Prior Knowledge. 26th Annual International Conference of the IEEE 1, 2004, pp 1648–1651
7. Chi Y: Automatic Segmentation of Cartilage in MR Images using CDCG: Chessboard Directional Compensated GVF Snakes. Medical Information Visualisation-BioMedical Visualisation (MediVis 2006), 2006, pp 45–50
8. Canny J: A Computational Approach to Edge Detection. IEEE Trans Pattern Anal Mach Intell PAMI-8:679–698, 1986
9. Huo YK, Wei G, Zhang YD, Wu LN: An Adaptive Threshold for the Canny Operator of Edge Detection. International Conference on Image Analysis and Signal Processing (IASP), 2010, pp 371–374
10. Harris C, Stephens M: A combined corner and edge detector. Proceedings of the 4th Alvey Vision Conference, 1988, pp 147–151
11. Protter, Murray H, Morrey Jr, Charles B: College Calculus with Analytic Geometry, 2nd edition. Addison-Wesley, LCCN, 1970, pp 520
12. Friedman JH: Another Approach to Polyehotomous Classification, Technical report, Stanford University, From:<http://www-stat.stanford.edu/~jhf/>, 1996
13. Rish, Irina: An empirical study of the naive Bayes classifier. IJCAI 2001 Workshop on Empirical Methods in Artificial Intelligence, 2001
14. Folkesson J, Dam E, Fogh Olsen O, Pettersen P, Christiansen C: Automatic segmentation of the articular cartilage in knee MRI using a hierarchical multi-class classification scheme. Med Image Comput Comput Assist Interv (MICCAI 2005) 327–334, 2005